ENVIRONMENTAL STUDIES

Cumulative risk of future bleaching for the world's coral reefs

Camille Mellin[1]*, Stuart Brown[1], Neal Cantin[2], Eduardo Klein-Salas[2], David Mouillot[3,4], Scott F. Heron[5], Damien A. Fordham[1]

Spatial and temporal patterns of future coral bleaching are uncertain, hampering global conservation efforts to protect coral reefs against climate change. Our analysis of daily projections of ocean warming establishes the severity, annual duration, and onset of severe bleaching risk for global coral reefs this century, pinpointing vital climatic refugia. We show that low-latitude coral regions are most vulnerable to thermal stress and will experience little reprieve from climate mitigation. By 2080, coral bleaching is likely to start on most reefs in spring, rather than late summer, with year-round bleaching risk anticipated to be high for some low-latitude reefs regardless of global efforts to mitigate harmful greenhouse gasses. By identifying Earth's reef regions that are at lowest risk of accelerated bleaching, our results will prioritize efforts to limit future loss of coral reef biodiversity.

INTRODUCTION

Coral reefs face some of the greatest and most urgent threats from climate change. Marine heatwaves that cause mass coral bleaching are increasing in frequency and spatial distribution as a result of human-induced climatic change, jeopardizing the survival of thousands of reef-associated organisms and the critical services they provide to nature and people (*1*, *2*). While coral bleaching events are set to intensify in coming decades (*3*, *4*), their spatial and temporal patterns remain uncertain, obstructing efforts to protect coral reefs against climate change.

Coral bleaching results from thermal stress, causing a breakdown of the symbiosis between the coral host and zooxanthellate microalgae (the family Symbiodiniaceae), leaving corals physiologically and nutritionally compromised (*5*). Corals ultimately die if temperature anomalies become too intense (>2°C) or persist for prolonged time periods. While the global risk of coral bleaching has increased by a rate of ca. 3.9% per annum in recent decades, owing to anthropogenic global warming (*6*), there is large spatial variation in these recent coral bleaching events (*6*, *7*). This indicates that some reef regions may be less exposed to future marine heatwaves. Pinpointing these safe havens for coral reefs is critical for deriving and strengthening conservation management and policy (*8*).

Current global patterns of future coral bleaching risk are hindered by coarse temporal resolution projections, narrowly focused metrics of thermal stress, and a general lack of on-ground validation. Existing forecasts are typically obtained from monthly (*3*, *9*, *10*) rather than daily projections of sea surface temperature (SST). This prevents important variations in daily temperatures from being captured in widely used indices of coral bleaching risk, including degree heating weeks [DHWs; °C-week (*11*)]. Consequently, the threat of cumulative heat stress from human-driven climate change for corals is poorly understood in space and time, affecting insights into the annual duration and timing of future onset of severe risk of coral bleaching across

Earth's oceans. This is despite these threats having potentially devastating impacts on coral biology that can impair the capacity of reef corals to recover between successive bleaching events (*12*, *13*). Thus, the absence of high spatiotemporal resolution projections of biologically relevant climatic threats to corals, not only restricts predictions of future risk of coral bleaching and associated mortality but also limits forecasts of coral recovery and their potential to adapt to warmer oceans. This includes determining whether oceanic warming is likely to cause coral bleaching to start coinciding with coral spawning events, which for some taxa is a single annual episode (*14*), having devastating impacts on coral recovery.

Here, we used daily global projections of SST derived from the Coupled Model Intercomparison Project Phase 6 (CMIP6) to project coral bleaching risk over a historical baseline period (1985–2014) and into the future (2015–2100) using two contrasting climate change scenarios, spatially mapped at 0.5° resolution (ca. 50 km). We downscaled and calibrated daily projections of SST using observed satellite data and validated these using a global database of historical bleaching records. We then derived multiple spatially explicit metrics of coral exposure to future heat stress, including (i) mean annual rate of increase in thermal stress, (ii) mean annual duration of thermal stress, and (iii) onset of thermal stress for coral reef locations globally. We show that the world's coral reefs will increasingly be exposed not only to greater heat stress but also to longer durations and earlier onsets of severe bleaching risk, with the highest cumulative bleaching risk being in regions of greatest coral diversity.

RESULTS

Uneven rates of increased future heat stress

Coral bleaching risk is commonly predicted from annual maximum DHW (DHW_{max}), for which we calculated the decadal trend (*15*) in each reef cell from 2015 to 2100 using multimodel ensemble averaged forecasts, according to two contrasting Shared Socioeconomic Pathways (SSPs). We project a mean increase in future thermal stress of 4.2°C-week decade^{-1} (equivalent to a decadal gain of 1 month of thermal stress at 1°C above normal summer maximum) for coral reefs globally under the high-emissions scenario (SSP5-8.5) that Earth has been closely tracking (*16*, *17*). We forecast particularly rapid decadal rates of increase in DHW_{max}, for the Red Sea and Hawaii, occurring at

1.2 times the global rate (Fig. 1). While in other provinces, such as Southeast Polynesia, the risk of coral bleaching is forecast to increase at considerably slower rates, being equal to 0.7 times that of the global average. Although emission reduction will moderate these rates of increase in DHW_{max} and its spatial variation between provinces (fig. S1), the ranking of high- to low-exposure regions will remain largely unchanged. In a likely SSP2-4.5 scenario (a middle of the road emissions scenario) (18), we project a mean increase in future thermal stress of 1.9°C-week decade^{-1}, with future heat stress remaining highest for the Red Sea and Hawaii and lowest for Southeast Polynesia (Fig. 1D).

Our projections of DHW_{max} indicate that, irrespective of the climate model (fig. S1) and scenario being considered, some tropical provinces will warm at much faster rates than other ocean regions, making them more vulnerable to coral bleaching in coming decades. As the severity of heat stress increases over time, so does the risk of coral mortality. However, the relationship between bleaching severity and mortality is not strictly linear because responses of coral communities to thermal stress can vary across successive bleaching events due to environmental filtering–previously termed "ecological memory" (19). We project that the maximum heat stress for corals reefs on Australia's Great Barrier Reef, including those observed during the 2016 El Niño mass bleaching event [DHW_{max} of 13.3°C-week (20)], will double by ~2050 in the absence of a concerted effort to reduce climate change causing emissions, which is in line with previous regional projections under SSP5-8.5 (21). This will leave little-to-no capacity for the maintenance of protective thermal regimes with moderate heat stress (12) and any adaptative capacity of corals and their symbionts (22, 23).
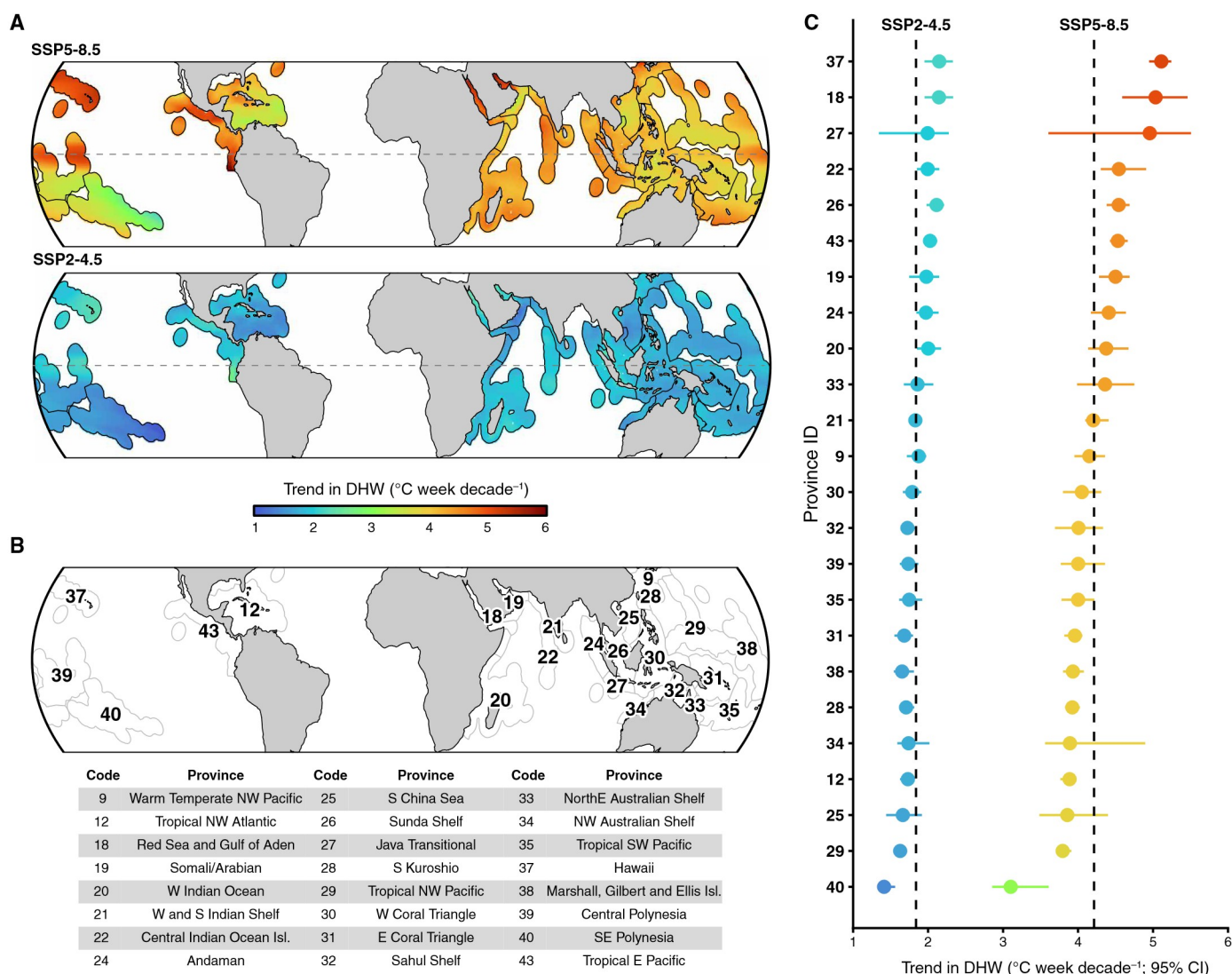
Fig. 1. Global rates of increase in bleaching severity. (A) Average decadal change in annual maximum DHWs (°C-week decade^{-1}) from 2015 to 2100 for mitigation (SSP2-4.5) and high-emissions (SSP5-8.5) scenarios. **(B)** Marine provinces with coral reefs (61). **(C)** Mean (dot) and 10th to 90th quantiles (error bar) of trend in DHW for each ecoregion shown in (B). The dotted lines indicate the global means for each climate scenario. Trend was calculated as the Sen's slope of annual DHW_{max} over time in each 0.5°-resolution coral reef grid cell. CI, confidence interval; NW, northwest; E, east; W, west; S, south; N, north; SE, southeast.

Code	Province	Code	Province	Code	Province
9	Warm Temperate NW Pacific	25	S China Sea	33	NorthE Australian Shelf
12	Tropical NW Atlantic	26	Sunda Shelf	34	NW Australian Shelf
18	Red Sea and Gulf of Aden	27	Java Transitional	35	Tropical SW Pacific
19	Somali/Arabian	28	S Kuroshio	37	Hawaii
20	W Indian Ocean	29	Tropical NW Pacific	38	Marshall, Gilbert and Ellis Isl.
21	W and S Indian Shelf	30	W Coral Triangle	39	Central Polynesia
22	Central Indian Ocean Isl.	31	E Coral Triangle	40	SE Polynesia
24	Andaman	32	Sahul Shelf	43	Tropical E Pacific

Longer exposures to severe bleaching

We quantified annual duration of severe bleaching risk as the total number of days with DHW $\geq$ 8°C-week (*11*) projected annually in each reef cell and according to each climate change scenario. Coral reefs at low latitudes are likely to be exposed to thermal stress levels related to severe bleaching for >3 months each year from as early as 2035 (Fig. 2A). By 2100, more than 50% of the world's reefs are expected to experience severe bleaching risk for >9 months per year under the SSP5-8.5 high-emissions scenario (Fig. 2B). Even with substantial mitigation of greenhouse gasses (SSP2-4.5), almost all of the world's coral reefs are likely to be exposed to >3 months of severe bleaching risk by 2080, with 20% of these reefs being exposed to severe bleaching conditions for >9 months of the year (Fig. 2B). Our projections align with previous modeling of marine heatwaves. While not specific to coral reefs, this modeling identified a 54% increase in annual marine heatwave days between 1925 and 2016 globally (*24*), with future projections predicting a near-constant heatwave state by the end of the century (*25*).

Annual exposure to heat stress was generally longer at low latitudes and along the equator (Fig. 2A). This reflects reduced seasonal variability in SST in the tropics compared to higher latitudes (*26*), with lower seasonal variability increasing the probability of bleaching occurring outside of the warmest season in these regions because SST is close to the bleaching threshold all year round. Our
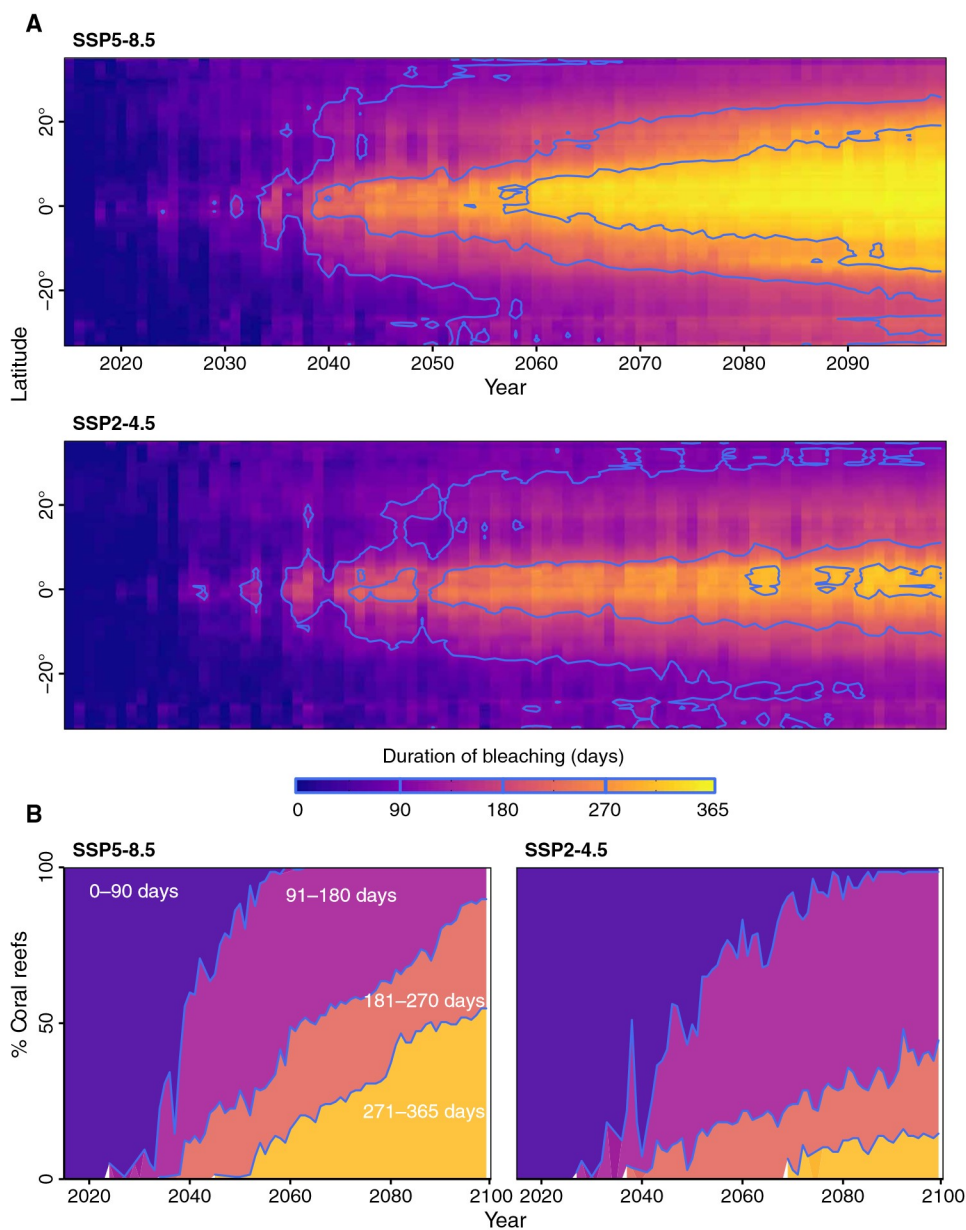

Fig. 2. Increasing duration of severe bleaching risk for the world's coral reefs. (**A**) Annual duration of severe bleaching risk (in days) at coral reef locations by latitude, year, and climate change scenario (SSP5-8.5 and SSP2-4.5). (**B**) Global proportion of coral reef cells (*n* = 72,744) affected by different durations of bleaching (0 to 90 days, 91 to 180 days, 181 to 270 days, and 271 to 365 days) in the 21st century in each climate change scenario.

forecasts of longer exposures to heat stress will likely induce further reductions in the return time of bleaching events (6), affecting the capability of corals to recover (12). Accordingly, it has previously been suggested that 2.7°C of global warming (which is forecast to occur by 2100 under SSP2-4.5) will cause high coral mortality even on reefs that currently experience little bleaching due to increased frequency in severity bleaching events (4). It can also be expected that longer exposure to heat stress in coming decades will increase the lethal effects of coral bleaching, overriding current-day sublethal effects on coral physiology and reproductive potential (27).

Earlier onset of bleaching risk

Defining the onset of severe bleaching risk as the number of days since mid-winter when DHW first exceeded the critical threshold of 8°C-week allowed us to quantify spatiotemporal variation in the onset of risk of coral bleaching. Using the climatological coldest day of the year (based on daily mean SST over the historical period of 1985–2012) as a mid-winter reference, we examined global variation in the timing of heat stress between hemispheres despite their opposing seasonality. This analysis shows that severe bleaching risk is generally predicted to start progressively earlier (considering mid-winter as the start of the year) over the course of the 21st century, with increased variability in the timing of heat stress increasing over time (Fig. 3).

Field observations (7) and satellite imagery (28) show that heat stress usually starts in late summer for most coral reef regions of the world. This is consistent with our multimodel ensemble baseline projections (fig. S2). However, by 2080, reefs in Central Polynesia and the Western Coral Triangle will likely experience severe bleaching risk from as early as late winter, with nearly all other reefs at low latitudes (and many at higher latitudes) experiencing severe bleaching from as early as spring. Spatial variation in the onset of bleaching risk is also likely to increase substantially in coming decades, with the world's coral reefs beginning to bleach in all seasons rather than just in late summer (Fig. 3). These forecasts indicate that the majority of Earth's reefs will experience onset conditions for bleaching in spring, and some in autumn, rather than late summer that is typical for most reefs today. We show that mitigating global emissions is likely to restrict timing of onset of severe bleaching risk to summer for most coral reefs (Fig. 3; SSP2-4.5).

An earlier onset of severe bleaching risk does not only increase the severity and duration of thermal stress but can also directly affect coral phenology, particularly if bleaching overlaps with key life cycle events such as coral spawning or larval recruitment. Reef corals produce some of the most spectacular mass reproductive events in the world. More than 130 species of corals on the Great Barrier Reef spawn only once a year, in a single week following a full moon in spring (14). Our analysis shows that by as early as 2040, this spawning event could coincide with severe bleaching risk, causing potential reproductive failure for these broadcast-spawning corals, increasing their extinction risk (29). While past observations of bleaching overlap with spawning events have remained rare (30), our analysis predicts that this will become much more common by the middle of this century.

Benefits of climate mitigation

Combining our three metrics of exposure to accumulated heat stress (severity: DHW_{max}; duration: number of days per year when
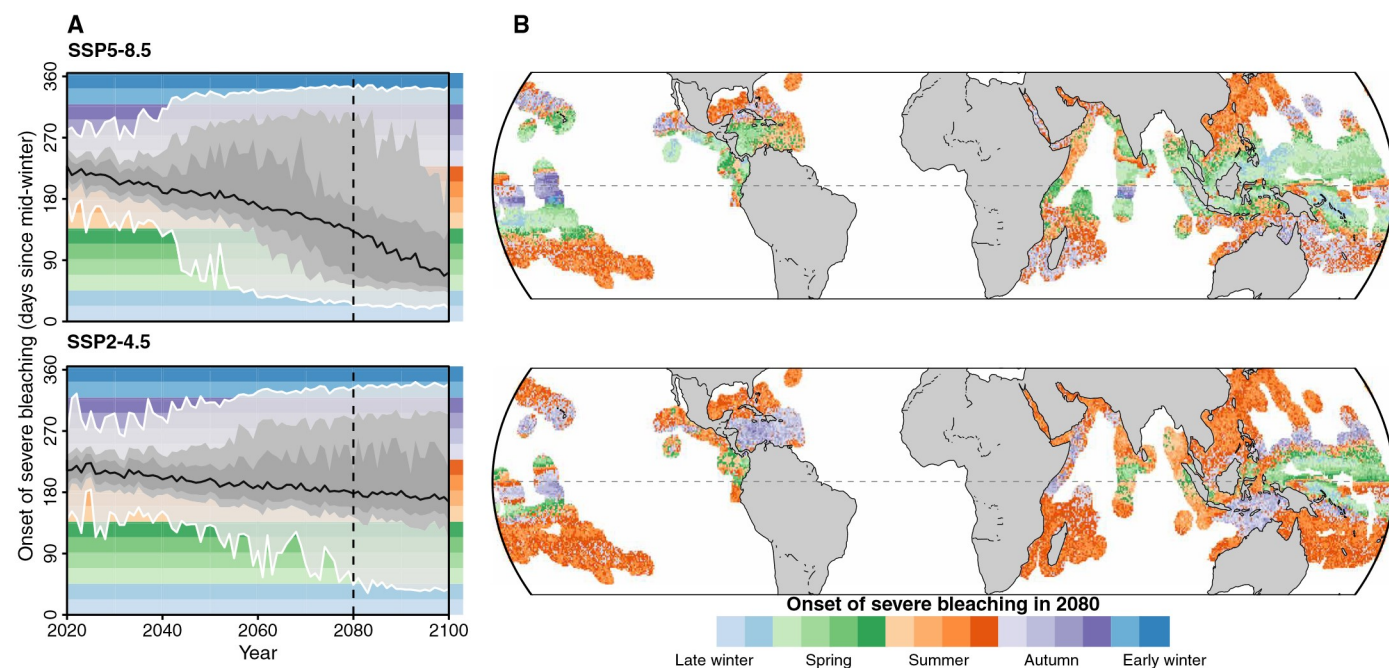
Fig. 3. Change in timing of severe bleaching risk. (**A**) Average timing of onset of severe bleaching for coral reefs globally (solid black line) and 10 to 90th, 25 to 75th, and 33 to 66th percentiles (ribbons) for two climate change scenarios. The horizontal bands represent months within season, with the reference (zero on the y axis) set to the middle of winter. (**B**) Onset of severe bleaching risk predicted within each reef cell by 2080 (i.e., averaged across the 2065–2095 period) according to each climate change scenario. Bleaching onset is defined as the number of days since mid-winter when severe bleaching is predicted in each grid cell (DHW ≥ 8°C-week). Predictions are based on a five-model ensemble.

DHW > 8°C-week; onset: number of days since mid-winter when DHW > 8°C-week) allowed us to predict cumulative bleaching risk in 2080 and compare it to the 2000 baseline under different climate mitigation scenarios. This composite metric combines the different deleterious effects and variable spatial patterns of the individual metrics (fig. S3). We used a principal components analysis (PCA) to reduce the dimensionality of these metrics, with the first two axes explaining 96.3% of the total variation in the three metrics combined (Fig. 4A). Close alignment of duration and severity of bleaching risk in the PCA indicates a corelationship, where greater accumulation of heat stress (severity) is typically associated with longer periods of heat stress (duration). We calculated cumulative risk for each coral reef grid cell as the Euclidean distance between its baseline position and its position under each future scenario on the two-dimensional (2D) PCA ordination plot (Fig. 4B). This allowed the benefit of mitigating

anthropogenic climate change to be assessed by calculating the Euclidean distance between ordination coordinates under SSP5-8.5 and SSP2-4.5 for each coral reef cell.

The highest cumulative risk of harmful bleaching and the lowest benefit of globally reducing greenhouse gasses occurred at low latitudes–particularly in the Eastern Coral Triangle, Marshall Islands, and Central Polynesia–indicating that coral reefs in equatorial regions will be disproportionately exposed to future risk of bleaching irrespective of the SSP considered (Fig. 4C), which aligns largely with latitudinal patterns of future heat stress predicted for corals using the older CMIP5 models (3, 31). Our finding of a reduced mitigation benefit at low latitudes was driven largely by projected increases in duration of severe bleaching risk, which remained large in both mitigation and high-emissions scenarios. At mid-latitudes, duration of severe bleaching risk decreased under SSP2-4.5. Other
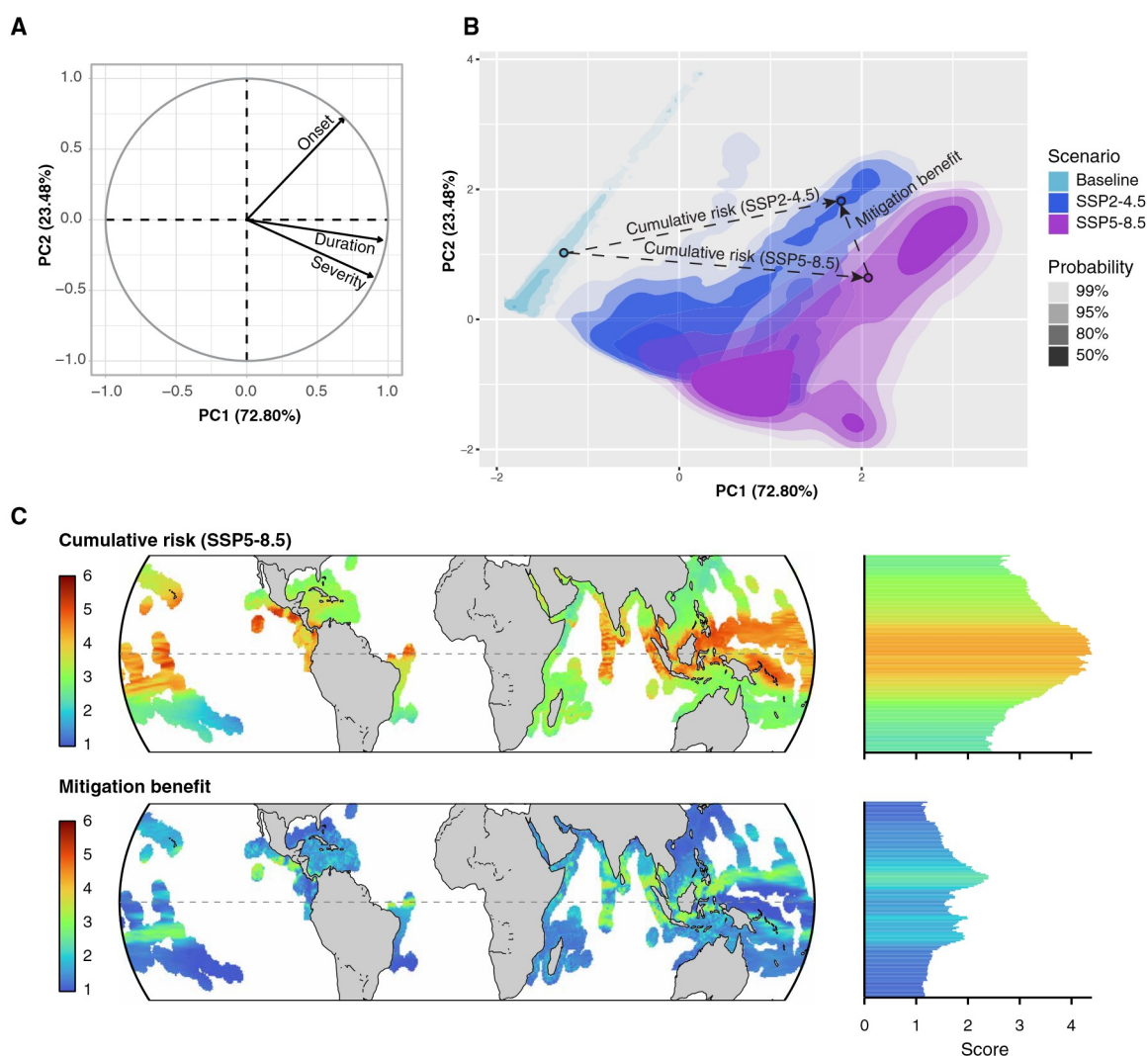

Fig. 4. Cumulative risk of future coral bleaching. (**A**) PCA of coral bleaching severity, duration and onset showing the variable ordination plot, and (**B**) individual ordination plot where each observation represents a coral reef grid cell (n = 72,744) exposed to the 2000 baseline or 2080 risk expected under the SSP2-4.5 or SSP5-8.5 climate scenario. Dashed arrows indicate the cumulative risk for an exemplar reef grid cell exposed to SSP2-4.5 and SSP5-8.5 risk, with the distance between the two future outcomes corresponding to the mitigation benefit. (**C**) Cumulative risk in 2080 based on SSP5-8.5 (top) and mitigation benefit expected under SSP2-4.5 (bottom), displayed as global (left) and latitudinal (right) patterns. PC, principal component.

metrics of severe bleaching risk showed relatively higher mitigation benefit along the equator (fig. S3).

Coral reefs at low latitudes host the highest levels of marine species richness and endemicity globally (32, 33). Greater cumulative risk of future bleaching at these global hot spots of marine biodiversity (34), combined with high risk of bleaching even under a climate pathway with reduced warming (SSP2-4.5), means that the most speciose coral reefs are disproportionally threatened by anthropogenic climate change. To compound matters, marine reef life in these areas are particularly ill-equipped to respond to accelerated rates of anthropogenic climate change, having been exposed only to relatively slow rates of climatic changes in the past (35). Furthermore, reefs in the Coral Triangle and Southwest Pacific Ocean, like many other low-latitude reefs, support the livelihoods and nutrition of local populations that still rely heavily on these resources for subsistence fishing (2, 36). Our finding that the highest climate impacts are expected in regions of highest social reliance on coral reefs (37) suggests that climate adaptation of fisheries and food systems in these regions should be an absolute priority.

Predictive ability of global climate models
Our downscaled projections of coral bleaching risk represent an important methodological advancement over past products for two major reasons. First, we used daily projections of SST, as opposed to monthly mean temperatures [e.g., (3, 9)], to calculate DHW. This ensured that high-frequency variability in SST contributed to the DHW calculation. Second, we bias-corrected our projections using the quantile delta mapping technique (38), which demonstrated superior skill in projecting bleaching risk compared to the more commonly applied delta change factor method [Supplementary Text; (39)].

Independent ecological validation of our high-resolution projections of coral bleaching risks, based on our multi-model ensemble hindcasts of severe bleaching risk (DHW ≥ 8°C-week), found that they were able to independently predict 90% of severe bleaching records that occurred from 1985 to 2010 (7). Further validation using high-resolution satellite monitoring data, showed a similar capacity for our modeled projections to reconcile observed bleaching conditions (fig. S4 and Supplementary Text) (40). These tests also showed that the multimodel averaged projection outperformed all individual model projections (fig. S5 and Supplementary Text) and were able to effectively distinguish bleaching from normal (nonbleaching) conditions (fig. S6 and Supplementary Text). This confirms the benefit of well-constructed, multimodel averaged climate projections for biodiversity assessments (41).

While other, more mechanistic approaches exist for downscaling SST that directly account for important regional oceanographic processes (9, 42), their global applications remain computationally intractable. However, recent developments in global shelf sea modeling approaches offer promising potential for semi-dynamic downscaling of climate projections, which could be applied to global extents (43). Therefore, our ecologically validated projections of coral bleaching provide a robust foundation for future assessments of the vulnerability of Earth's corals reefs to climate change, with strong application to ecological and fisheries modeling and management (see the "Data and materials availability" section in Acknowledgments).

DISCUSSION
Our validated analysis of daily SST projections revealed high spatiotemporal variation in the severity, annual duration, and onset of severe

bleaching conditions for Earth's coral reefs this century. We show that the most biodiversity rich coral regions are the most vulnerable to heat stress and that reef corals in these regions are likely to benefit least from global efforts to mitigate climate change. By 2080, substantially longer periods of heat stress are projected to cause the onset of coral bleaching to shift from late summer to spring in most coral reef regions. These projected changes will cause coral bleaching to overlap with key stages of the coral life cycle, including spawning and recruitment, resulting in potentially irreversible outcomes on population dynamics, culminating in widescale loss of corals.

Our results also pinpoint potential climate refugia at spatial scales that are directly relevant to coral reef conservation and management (ca. 50 km) (fig. S7). For example, within the tropical northwest Atlantic province, we predict much lower than average cumulative bleaching risk on the northern coasts of Venezuela and Colombia. Here, seasonal upwellings occur (44), bringing cooler water up to the ocean surface and potentially buffering extreme temperature anomalies that cause bleaching. Other less impacted areas include Socotra Island opposite the Gulf of Aden and Alor Kecil in Indonesia where upwellings are also prevalent (fig. S7). High spatial variability in cumulative bleaching risk also occurs in the Western Coral Triangle, but not for the Great Barrier Reef or Hawaii provinces (fig. S7). Although uncertainty remains regarding responses of oceanographic currents to anthropogenic climate change, our projections suggest that upwellings could continue to provide important climate refugia to coral reefs in warming oceans.

While our bleaching risk framework does not currently account for any coral adaptation to warming seas because it remains largely unknown or unquantified [but see (22)], coral adaptation over time could in theory be built into this framework by allowing the bleaching threshold to progressively increase over time (45). This coral adaptive capacity would likely provide greatest benefit in the equatorial regions projected to have the greatest risk of coral bleaching. Looking ahead, it will be important to account for other primary threats to coral reefs, such as ocean acidification or tropical cyclones (46, 47), and their cumulative impacts (48–50) using similar frameworks. Our modeling framework also offers a platform to implement additional climate models and scenarios as required. Our choice of climate change scenarios was driven by the need to include the most likely SSP (SSP2-4.5) (18), and a worst-case, yet still plausible scenario for comparison and conservation decision making [SSP5-8.5; (17, 51)], noting that thermal stress levels predicted for the Northwest Atlantic by 2040 under SSP5-8.5 (fig. S1) have already been exceeded (16).

Curbing greenhouse gas emissions is ultimately the only solution to limit the frequency and severity of coral exposure to heat stress. While these mitigation efforts will only partially slow the rise of severe bleaching risk in coral reef ecosystems, they could be vital for preserving some corals and reefs. Alternative local-to-regional coral conservation strategies are also needed to prevent widescale coral loss. Irrespective of whether these interventions involve assisted evolution, coral translocation, or coral restoration (52, 53), success will be maximized in spatial refugia characterized by lower regional cumulative risk of bleaching.

MATERIALS AND METHODS
Experimental design
Climate data processing and DHW calculation
An overview of the climate processing and database creation is presented in fig. S8 and fully detailed in (39). Briefly, daily simulated

SSTs from eight Atmosphere-Ocean General Circulation Models (AOGCMs) were accessed from the CMIP6 (*54*) for the period 1985 to 2100 for two SSPs (*55*): SSP2-4.5 and SSP5-8.5. Data were downscaled to a 0.5° × 0.5° regular grid and bias-corrected against a high-resolution SST satellite dataset (*56*) using the quantile delta mapping technique (*38*). Downscaled and bias-corrected data were used to calculate: (i) estimates of daily SST; (ii) SST summertime anomalies (a.k.a. hot spots; °C) above a spatially resolved bleaching threshold [defined as the maximum monthly mean (MMM) SST] (*11*); and (iii) cumulative heat stress defined as DHWs (DHW, °C-week), calculated as the cumulative sum of hot spots above the MMM for each pixel over a rolling 12-week (84-day) window.

We generated a multimodel ensemble average based on five CMIP6 models that had a transient climate response (i.e., warming from a simulation that is driven by an exponential 1.0% per year increase in CO_2) inside the 1.4° to 2.2°C range as recommended by Hausfather *et al.* (*57*) (table S1). It has previously been shown that the skill of multimodel averaged ensemble climate projections tends to approach an asymptote after approximately 5 different models have been averaged together (*58*), suggesting that adding any more models is unlikely to improve multimodel ensemble skill. For individual model projections and for the five-model ensemble (*ens5*), we excluded non-reef grid cells from subsequent index calculations based on the National Oceanic Atmospheric Administration Coral Reef Watch reef locations dataset (*59*).

We validated our global climatological daily mean bias-corrected SST hindcasts by comparing them to a high-resolution satellite-derived SST dataset (*56*), which was created as part of the European Space Agency SST Climate Change Initiative (CCI) (hereafter CCI analysis SST) (*40*) available as an open access dataset at https://data.ceda.ac.uk/neodc/esacci/sst/data/CDR_v2/Analysis/L4/v2.1. Full details of the climatological validation are given in (*39*).

An intermodel comparison showed that decadal trends in DHW_{max} were highly consistent among the five individual CMIP6 AOGCMs used to calculate ensemble averaged forecasts of DHW_{max} for each scenario (fig. S1), providing good confidence in our multimodel ensemble projections. Moreover, the ensemble decadal trend in DHW_{max} strongly correlated with the mean DHW_{max} forecast by 2080 in each grid cell (fig. S9), which we therefore included in our cumulative risk index described below.

Synoptic metrics of exposure to heat stress

For each emission scenario, we calculated the decadal trend in future bleaching risk in each coral reef pixel as the Theil-Sen's median slope (*15, 60*) of DHW over the 2015–2100 time period based on the five-model ensemble, as well as on individual models. We then aggregated Theil-Sen's slopes at the province level to derive the median, 10th and 90th percentiles. Provinces were extracted from the Marine Ecoregions of the World dataset (*61*) after excluding provinces with <5 reef grid cells.

We calculated the magnitude, duration, and onset of heat stress expected by 2080 in each coral reef pixel, according to each emission scenario and based on the five-model ensemble as the average of each metric over 2065–2095. The magnitude of heat stress was defined as the annual DHW_{max} expected within each pixel and averaged over 2065–2095. The duration of heat stress was defined as the annual number of days when DHW exceeded 8°C-week [i.e., bleaching alert level 2 for a minimum of 1 day, (*11*)] averaged over 2065–2095.

The onset of heat stress was defined as the first annual occurrence of DHW above the 8°C-week threshold. To control for differences in seasonality between hemispheres, we set the reference for this calculation to the climatological coldest day of the year in each pixel and calculated the onset as the number of days since the climatological coldest when DHW exceeded 8°C-week. The climatological coldest day of the year was identified for each pixel based on each model's historical projections between 1985 and 2012. To match the onset of heat stress to its respective season in each pixel, we considered the climatological coldest of the year as the middle of winter, with winter encompassing ±45 days of the climatological coldest day, followed by 90 days of spring, summer, and autumn, respectively.

Statistical analysis
Cumulative risk index
We defined a cumulative risk index by combining our three metrics of heat stress averaged over 2065–2095 (magnitude: annual DHW_{max}; duration: number of days when DHW ≥ 8°C-week; onset: day of the year relative to coldest when DHW ≥ 8°C-week) for each climate scenario and for the baseline period (1985–2014). Standardization of the three metrics was undertaken by subtracting their mean and dividing by their standard deviation. Metrics were combined using a PCA, with the first two axes explaining 96.3% of the total variation in these metrics (Fig. 4A).

We calculated the cumulative risk for each coral reef grid cell as the Euclidean distance between its baseline position, and its position under each climate scenario on the PCA 2D ordination plot (Fig. 4B). The climate mitigation benefit for that reef grid cell corresponds to the Euclidean distance between its ordination coordinates under SSP5-8.5 and SSP2-4.5 (Fig. 4B).

Before the PCA, we cosine-transformed the onset to convert it from Julian days to the [−1;1] scale (fig. S10). This allowed us to achieve two outcomes: (i) obtain similar onset values for days 1 and 365 of the Julian calendar (consecutive dates within the same season) and (ii) an onset in day 1 (mid-winter) receives a cosine-transformed value of 1 (highest threat), and an onset in day 187 (mid-summer) receives a cosine-transformed value of −1 (lowest threat), thus making the ranking of value from low to high threats comparable to other metrics.

Ecological validation
We tested the ability of our DHW projections to predict the occurrence of severe bleaching records between 1985 and 2010 (*7*) in each of the IPCC AR6 Working Group 1 reference regions (*62*). We did this by calculating the hit rate (*63*) as the proportion of severe bleaching records correctly predicted by each of the CMIP6 models and the *ens5* ensemble, as well as the CCI analysis SST, i.e., where DHW ≥ 4°C-week within 18 months of an observed bleaching record for each dataset. For this analysis, observed bleaching records were pooled within each 0.5° grid cell, thus reducing the influence of multiple records corresponding to the same bleaching event in each grid cell. Full details for this calculation are given in (*39*).

We used beta regression (*64*) to test for differences in the hit rate between our *ens5* ensemble and the CCI analysis SST as the number of bleaching records increased. Models were constructed with normal priors ($\beta_k \sim Normal(0,2.5)$) and four chains, each with 2000 samples, with the first 1000 samples being discarded as burn-in. We ensured model convergence using Gelman-Rubin statistics (where values less than or equal to 1.1 were considered acceptable), along with testing for effective sample size, and visually examining trace plots. We performed posterior predictive checks to evaluate the model predictive accuracy relative to the observed data. The analysis was performed

using the rstanarm package in R (65). We plotted and compared the distribution of DHW values matching severe bleaching records with those within 1985–2012 at the same locations (i.e., baseline period) for both the *ens5* hindcast and the CCI analysis.

Last, we compared the spatial coverage for our onset metric in 2000 (averaged over 1985–2015) to that derived from satellite analysis (28) from the same period. Because not all reefs were exposed to bleaching alert level 2 during this period according to either dataset, we used a threshold of DHW $\geq$ 4°C-week (bleaching alert level 1; excluding non-reef cells) to verify that patterns of the onset predicted in 2000 were similar across datasets (fig. S2).

Supplementary Materials

This PDF file includes:
Supplementary Text
Figs. S1 to S10
Table S1

REFERENCES AND NOTES

1. T. P. Hughes, M. L. Barnes, D. R. Bellwood, J. E. Cinner, G. S. Cumming, J. B. C. Jackson, J. Kleypas, I. A. van de Leemput, J. M. Lough, T. H. Morrison, S. R. Palumbi, E. H. van Nes, M. Scheffer, Coral reefs in the Anthropocene. *Nature* **546**, 82–90 (2017).
2. C. Mellin, C. Hicks, D. A. Fordham, C. Golden, M. Kjellevold, M. A. MacNeil, E. Maire, S. Mangubhai, D. Mouillot, K. L. Nash, J. O. Omukoto, J. P. W. Robinson, R. D. Stuart-Smith, J. Zamborain-Mason, G. Edgar, N. A. J. Graham, Safeguarding nutrients from coral reefs under climate change. *Nat. Ecol. Evol.* **6**, 1808–1817 (2022).
3. R. van Hooidonk, J. Maynard, J. Tamelander, J. Gove, G. Ahmadia, L. Raymundo, G. Williams, S. F. Heron, S. Planes, Local-scale projections of coral reef futures and implications of the Paris Agreement. *Sci. Rep.* **6**, 39666 (2016).
4. A. M. Dixon, P. M. Forster, S. F. Heron, A. M. K. Stoner, M. Beger, Future loss of local-scale thermal refugia in coral reef ecosystems. *PLOS Climate* **1**, e0000004 (2022).
5. P. W. Glynn, Widespread coral mortality and the 1982–83 El Niño warming event. *Environ. Conserv.* **11**, 133–146 (1984).
6. T. P. Hughes, K. D. Anderson, S. R. Connolly, S. F. Heron, J. T. Kerry, J. M. Lough, A. H. Baird, J. K. Baum, M. L. Berumen, T. C. Bridge, D. C. Claar, C. M. Eakin, J. P. Gilmour, N. A. J. Graham, H. Harrison, J.-P. A. Hobbs, A. S. Hoey, M. Hoogenboom, R. J. Lowe, M. T. McCulloch, J. M. Pandolfi, M. Pratchett, V. Schoepf, G. Torda, S. K. Wilson, Spatial and temporal patterns of mass bleaching of corals in the Anthropocene. *Science* **359**, 80–83 (2018).
7. S. D. Donner, G. J. M. Rickbeil, S. F. Heron, A new, high-resolution global mass coral bleaching database. *PLOS ONE* **12**, e0175490 (2017).
8. O. Hoegh-Guldberg, E. V. Kennedy, H. L. Beyer, C. McClennen, H. P. Possingham, Securing a long-term future for coral reefs. *Trends Ecol. Evol.* **33**, 936–944 (2018).
9. R. van Hooidonk, J. A. Maynard, Y. Liu, S.-K. Lee, Downscaled projections of Caribbean coral bleaching that can inform conservation planning. *Glob. Chang. Biol.* **21**, 3389–3401 (2015).
10. H. L. Beyer, E. V. Kennedy, M. Beger, C. A. Chen, J. E. Cinner, E. S. Darling, C. M. Eakin, R. D. Gates, S. F. Heron, N. Knowlton, D. O. Obura, S. R. Palumbi, H. P. Possingham, M. Puotinen, R. K. Runting, W. J. Skirving, M. Spalding, K. A. Wilson, S. Wood, J. E. Veron, O. Hoegh-Guldberg, Risk-sensitive planning for conserving coral reefs under rapid climate change. *Conserv. Lett.* **11**, e12587 (2018).
11. G. Liu, S. Heron, C. M. Eakin, F. Muller-Karger, M. Vega-Rodriguez, L. Guild, J. De La Cour, E. Geiger, W. Skirving, T. Burgess, A. Strong, A. Harris, E. Maturi, A. Ignatov, J. Sapper, J. Li, S. Lynds, Reef-scale thermal stress monitoring of coral ecosystems: New 5-km global products from NOAA coral reef watch. *Remote Sens.* **6**, 11579–11606 (2014).
12. T. D. Ainsworth, S. F. Heron, J. C. Ortiz, P. J. Mumby, A. Grech, D. Ogawa, C. M. Eakin, W. Leggat, Climate change disables coral bleaching protection on the Great Barrier Reef. *Science* **352**, 338–342 (2016).
13. R. van Woesik, T. Shlesinger, A. G. Grottoli, R. J. Toonen, R. Vega Thurber, M. E. Warner, A. Marie Hulver, L. Chapron, R. H. McLachlan, R. Albright, E. Crandall, T. M. DeCarlo, M. K. Donovan, J. Eirin-Lopez, H. B. Harrison, S. F. Heron, D. Huang, A. Humanes, T. Krueger, J. S. Madin, D. Manzello, L. C. McManus, M. Matz, E. M. Muller, M. Rodriguez-Lanetty, M. Vega-Rodriguez, C. R. Voolstra, J. Zaneveld, Coral-bleaching responses to climate change across biological scales. *Glob. Chang. Biol.* **28**, 4229–4250 (2022).
14. S. A. Keith, J. A. Maynard, A. J. Edwards, J. R. Guest, A. G. Bauman, R. van Hooidonk, S. F. Heron, M. L. Berumen, J. Bouwmeester, S. Piromvaragorn, C. Rahbek, A. H. Baird, Coral

15. P. K. Sen, Estimates of the regression coefficient based on Kendall's Tau. *J. Am. Stat. Assoc.* **63**, 1379–1389 (1968).
16. O. Hoegh-Guldberg, W. Skirving, S. G. Dove, B. L. Spady, A. Norrie, E. F. Geiger, G. Liu, J. L. De La Cour, D. P. Manzello, Coral reefs in peril in a record-breaking year. *Science* **382**, 1238–1240 (2023).
17. C. R. Schwalm, S. Glendon, P. B. Duffy, RCP8.5 tracks cumulative CO2 emissions. *Proc. Natl. Acad. Sci. U.S.A.* **117**, 19656–19657 (2020).
18. R. Pielke Jr., M. G. Burgess, J. Ritchie, Plausible 2005–2050 emissions scenarios project between 2 °C and 3 °C of warming by 2100. *Environ. Res. Lett.* **17**, 024027 (2022).
19. T. P. Hughes, J. T. Kerry, S. R. Connolly, J. G. Álvarez-Romero, C. M. Eakin, S. F. Heron, M. A. Gonzalez, J. Moneghetti, Emergent properties in the responses of tropical corals to recurrent climate extremes. *Curr. Biol.* **31**, 5393–5399.e3 (2021).
20. N. E. Cantin, E. Klein-Salas, P. R. Frade, *Spatial variability in coral bleaching severity and mortality during the 2016 and 2017 Great Barrier Reef coral bleaching events.* Report to the National Environmental Science Program (Reef and Rainforest Research Centre Limited, 2021), 64 pp.
21. J. K. McWhorter, P. R. Halloran, G. Roff, W. J. Skirving, C. T. Perry, P. J. Mumby, The importance of 1.5°C warming for the Great Barrier Reef. *Glob. Chang. Biol.* **28**, 1332–1341 (2022).
22. C. A. Logan, J. P. Dunne, J. S. Ryan, M. L. Baskett, S. D. Donner, Quantifying global potential for coral evolutionary response to climate change. *Nat. Clim. Chang.* **11**, 537–542 (2021).
23. C. E. Cornwall, S. Comeau, S. D. Donner, C. Perry, J. Dunne, R. van Hooidonk, J. S. Ryan, C. A. Logan, Coral adaptive capacity insufficient to halt global transition of coral reefs into net erosion under climate change. *Glob. Chang. Biol.* **29**, 3010–3018 (2023).
24. E. C. J. Oliver, M. G. Donat, M. T. Burrows, P. J. Moore, D. A. Smale, L. V. Alexander, J. A. Benthuysen, M. Feng, A. Sen Gupta, A. J. Hobday, N. J. Holbrook, S. E. Perkins-Kirkpatrick, H. A. Scannell, S. C. Straub, T. Wernberg, Longer and more frequent marine heatwaves over the past century. *Nat. Commun.* **9**, 1324 (2018).
25. E. C. J. Oliver, M. T. Burrows, M. G. Donat, A. Sen Gupta, L. V. Alexander, S. E. Perkins-Kirkpatrick, J. A. Benthuysen, A. J. Hobday, N. J. Holbrook, P. J. Moore, M. S. Thomsen, T. Wernberg, D. A. Smale, Projected marine heatwaves in the 21st century and the potential for ecological impact. *Front. Mar. Sci.* **6**, 734 (2019).
26. P. K. Dunstan, S. D. Foster, E. King, J. Risbey, T. J. O'Kane, D. Monselesan, A. J. Hobday, J. R. Hartog, P. A. Thompson, Global patterns of change and variation in sea surface temperature and chlorophyll a. *Sci. Rep.* **8**, 14624 (2018).
27. S. E. Leinbach, K. E. Speare, A. M. Rossin, D. M. Holstein, M. E. Strader, Energetic and reproductive costs of coral recovery in divergent bleaching responses. *Sci. Rep.* **11**, 23546 (2021).
28. S. F. Heron, J. A. Maynard, R. van Hooidonk, C. M. Eakin, Warming trends and bleaching stress of the world's coral reefs 1985-2012. *Sci. Rep.* **6**, 38402 (2016).
29. T. Shlesinger, Y. Loya, Breakdown in spawning synchrony: A silent threat to coral persistence. *Science* **365**, 1002–1007 (2019).
30. T. Foster, A. J. Heyward, J. P. Gilmour, Split spawning realigns coral reproduction with optimal environmental windows. *Nat. Commun.* **9**, 718 (2018).
31. N. H. Wolff, S. D. Donner, L. Cao, R. Iglesias-Prieto, P. F. Sale, P. J. Mumby, Global inequities between polluters and the polluted: Climate change impacts on coral reefs. *Glob. Chang. Biol.* **21**, 3982–3994 (2015).
32. D. R. Bellwood, T. Hughes, Regional-scale assembly rules and biodiversity of coral reefs. *Science* **292**, 1532–1535 (2001).
33. T. P. Hughes, D. R. Bellwood, S. R. Connolly, Biodiversity hotspots, centres of endemicity, and the conservation of coral reefs. *Ecol. Lett.* **5**, 775–784 (2002).
34. F. Ramírez, I. Afán, L. S. Davis, A. Chiaradia, Climate impacts on global hot spots of marine biodiversity. *Sci. Adv.* **3**, e1601198 (2017).
35. S. C. Brown, C. Mellin, J. García Molinos, E. D. Lorenzen, D. A. Fordham, Faster ocean warming threatens richest areas of marine biodiversity. *Glob. Chang. Biol.* **28**, 5849–5858 (2022).
36. J. Barlow, F. França, T. A. Gardner, C. C. Hicks, G. D. Lennox, E. Berenguer, L. Castello, E. P. Economo, J. Ferreira, B. Guénard, C. Gontijo Leal, V. Isaac, A. C. Lees, C. L. Parr, S. K. Wilson, P. J. Young, N. A. J. Graham, The future of hyperdiverse tropical ecosystems. *Nature* **559**, 517–526 (2018).
37. T. D. Ainsworth, W. Leggat, B. R. Silliman, C. A. Lantz, J. L. Bergman, A. J. Fordyce, C. E. Page, J. J. Renzi, J. Morton, C. M. Eakin, S. F. Heron, Rebuilding relationships on coral reefs: Coral bleaching knowledge-sharing to aid adaptation planning for reef users. *Bioessays* **43**, e2100048 (2021).
38. A. J. Cannon, S. R. Sobie, T. Q. Murdock, Bias correction of GCM precipitation by quantile mapping: How well do methods preserve changes in quantiles and extremes? *J. Climate* **28**, 6938–6959 (2015).
39. C. Mellin, S. C. Brown, S. Heron, D. A. Fordham, CoralBleachRisk- Global projections of coral bleaching risk in the 21st century. bioRxiv 589829 [Preprint]. 24 April 2024. https://doi.org/10.1101/2024.04.16.589829.

40. S. A. Good, O. Embury, C. E. Bulgin, J. Mittaz, *ESA Sea Surface Temperature Climate Change Initiative (SST_cci): Level 4 Analysis Climate Data Record, version 2.1* (CEDA, 2019); http://dx.doi.org/10.5285/62c0f97b1eac4e0197a674870afe1ee6.

41. D. A. Fordham, T. M. Wigley, B. W. Brook, Multi-model climate projections for biodiversity risk assessments. *Ecol. Appl.* **21**, 3317–3331 (2011).

42. J. K. McWhorter, P. R. Halloran, G. Roff, W. J. Skirving, P. J. Mumby, Climate refugia on the Great Barrier Reef fail when global warming exceeds 3°C. *Glob. Chang. Biol.* **28**, 5768–5780 (2022).

43. P. R. Halloran, J. K. McWhorter, B. Arellano Nava, R. Marsh, W. Skirving, S2P3-R v2.0: Computationally efficient modelling of shelf seas on regional to global scales. *Geosci. Model Dev.* **14**, 6177–6195 (2021).

44. C. A. Andrade, E. D. Barton, The Guajira upwelling system. *Cont. Shelf Res.* **25**, 1003–1022 (2005).

45. C. A. Logan, J. P. Dunne, C. M. Eakin, S. D. Donner, Incorporating adaptive responses into future projections of coral bleaching. *Glob. Chang. Biol.* **20**, 125–139 (2014).

46. R. O. Setter, E. C. Franklin, C. Mora, Co-occurring anthropogenic stressors reduce the timeframe of environmental viability for the world's coral reefs. *PLOS Biol.* **20**, e3001821 (2022).

47. S. G. Klein, N. R. Geraldi, A. Anton, S. Schmidt-Roach, M. Ziegler, M. J. Cziesielski, C. Martin, N. Rädecker, T. L. Frölicher, P. J. Mumby, J. M. Pandolfi, D. J. Suggett, C. R. Voolstra, M. Aranda, C. M. Duarte, Projecting coral responses to intensifying marine heatwaves under ocean acidification. *Glob. Chang. Biol.* **28**, 1753–1765 (2022).

48. F. J. González-Barrios, N. Estrada-Saldívar, E. Pérez-Cervantes, F. Secaira-Fajardo, L. Álvarez-Filip, Legacy effects of anthropogenic disturbances modulate dynamics in the world's coral reefs. *Glob. Chang. Biol.* **29**, 3285–3303 (2023).

49. M. A. MacNeil, C. Mellin, S. Matthews, N. H. Wolff, T. R. McClanahan, M. Devlin, C. Drovandi, K. Mengersen, N. A. J. Graham, Water quality mediates resilience on the Great Barrier Reef. *Nat. Ecol. Evol.* **3**, 620–627 (2019).

50. C. Mellin, S. Matthews, K. R. N. Anthony, S. C. Brown, M. J. Caley, K. Johns, K. Osborne, M. Puotinen, A. Thompson, N. H. Wolff, D. A. Fordham, M. A. MacNeil, Spatial resilience of the Great Barrier Reef under cumulative disturbance impacts. *Glob. Chang. Biol.* **25**, 2431–2445 (2019).

51. V. Hemming, A. E. Camaclang, M. S. Adams, M. Burgman, K. Carbeck, J. Carwardine, I. Chadès, L. Chalifour, S. J. Converse, L. N. K. Davidson, G. E. Garrard, R. Finn, J. R. Fleri, J. Huard, H. J. Mayfield, E. M. Madden, I. Naujokaitis-Lewis, H. P. Possingham, L. Rumpff, M. C. Runge, D. Stewart, V. J. D. Tulloch, T. Walshe, T. G. Martin, An introduction to decision science for conservation. *Conserv. Biol.* **36**, e13868 (2022).

52. Z. L. Fuller, V. J. L. Mocellin, L. A. Morris, N. Cantin, J. Shepherd, L. Sarre, J. Peng, Y. Liao, J. Pickrell, P. Andolfatto, M. Matz, L. K. Bay, M. Przeworski, Population genetics of the coral Acropora millepora: Toward genomic prediction of bleaching. *Science* **369**, eaba4674 (2020).

53. M. J. H. van Oppen, R. D. Gates, L. L. Blackall, N. Cantin, L. J. Chakravarti, W. Y. Chan, C. Cormick, A. Crean, K. Damjanovic, H. Epstein, P. L. Harrison, T. A. Jones, M. Miller, R. J. Pears, L. M. Peplow, D. A. Raftos, B. Schaffelke, K. Stewart, G. Torda, D. Wachenfeld, A. R. Weeks, H. M. Putnam, Shifting paradigms in restoration of the world's coral reefs. *Glob. Chang. Biol.* **23**, 3437–3448 (2017).

54. V. Eyring, S. Bony, G. A. Meehl, C. A. Senior, B. Stevens, R. J. Stouffer, K. E. Taylor, Overview of the Coupled Model Intercomparison Project Phase 6 (CMIP6) experimental design and organization. *Geosci. Model Dev.* **9**, 1937–1958 (2016).

55. B. C. O'Neill, E. Kriegler, K. L. Ebi, E. Kemp-Benedict, K. Riahi, D. S. Rothman, B. J. van Ruijven, D. P. van Vuuren, J. Birkmann, K. Kok, M. Levy, W. Solecki, The roads ahead: Narratives for shared socioeconomic pathways describing world futures in the 21st century. *Glob. Environ. Chang.* **42**, 169–180 (2017).

56. C. J. Merchant, O. Embury, C. E. Bulgin, T. Block, G. K. Corlett, E. Fiedler, S. A. Good, J. Mittaz, N. A. Rayner, D. Berry, S. Eastwood, M. Taylor, Y. Tsushima, A. Waterfall, R. Wilson, C. Donlon, Satellite-based time-series of sea-surface temperature since 1981 for climate applications. *Sci. Data* **6**, 223 (2019).

57. Z. Hausfather, K. Marvel, G. A. Schmidt, J. W. Nielsen-Gammon, M. Zelinka, Climate simulations: Recognize the 'hot model' problem. *Nature* **605**, 26–29 (2022).

58. D. W. Pierce, T. P. Barnett, B. D. Santer, P. J. Gleckler, Selecting global climate models for regional climate change studies. *Proc. Natl. Acad. Sci. U.S.A.* **106**, 8441–8446 (2009).

59. S. F. Heron, L. Johnston, G. Liu, E. F. Geiger, J. A. Maynard, J. L. De La Cour, S. Johnson, R. Okano, D. Benavente, T. F. R. Burgess, J. Iguel, D. I. Perez, W. J. Skirving, A. E. Strong, K. Tirak, C. M. Eakin, Validation of Reef-Scale Thermal Stress Satellite Products for Coral Bleaching Monitoring. *Remote Sens.* **8**, 59 (2016).

60. H. Theil, A rank-invariant method of linear and polynomial regression analysis in *Henri Theil's Contributions to Economics and Econometrics: Econometric Theory and Methodology*, B. Raj, J. Koerts, Eds. (Springer, 1992), pp. 345–381.

61. M. D. Spalding, H. E. Fox, G. R. Allen, N. Davidson, Z. A. Ferdaña, M. Finlayson, B. S. Halpern, M. A. Jorge, A. Lombana, S. A. Lourie, K. D. Martin, E. McManus, J. Molnar, C. A. Recchia, J. Robertson, Marine ecoregions of the world: A bioregionalization of coastal and shelf areas. *Bioscience* **57**, 573–583 (2007).

62. M. Iturbide, J. M. Gutiérrez, L. M. Alves, J. Bedia, R. Cerezo-Mota, E. Cimadevilla, A. S. Cofiño, A. Di Luca, S. H. Faria, I. V. Gorodetskaya, M. Hauser, S. Herrera, K. Hennessy, H. T. Hewitt, R. G. Jones, S. Krakovska, R. Manzanas, D. Martínez-Castro, G. T. Narisma, I. S. Nurhati, I. Pinto, S. I. Seneviratne, B. van den Hurk, C. S. Vera, An update of IPCC climate reference regions for subcontinental analysis of climate model data: Definition and aggregated datasets. *Earth Syst. Sci. Data* **12**, 2959–2970 (2020).

63. C. M. Spillman, G. A. Smith, A new operational seasonal thermal stress prediction tool for coral reefs around Australia. *Front. Mar. Sci.* **8**, (2021).

64. S. Ferrari, F. Cribari-Neto, Beta regression for modelling rates and proportions. *J. Appl. Stat.* **31**, 799–815 (2004).

65. A. Gelman, B. Goodrich, J. Gabry, A. Vehtari, R-squared for bayesian regression models. *Am. Statist.* **73**, 307–309 (2018).